

---

# A Singularity Solution to the Effect of the Axial Velocity Ratio on the Cascade Performance and its Design Application

---

**WEI Binghai and WU Keqi**

*Power Engineering Dept.,  
Huazhong Univ. of Sci. and  
Tech., Wuhan,  
China, 430074*

**Abstract:** A singularity solution to the effect of the axial velocity ratio on the cascade performance based on Schlichting theory is presented in this paper. The flow angle data calculated by this theoretical correcting method shows a good agreement with experimental ones. Employing the singularity method can result in a development of the conventional design procedure using NACA cascade data. The validity and reliability of the singularity solution and the improved design procedure is indicated by two design examples.

---

## INTRODUCTION

A design procedure of axial (or diagonal) flow fan using NACA cascade data usually implicates and demands an assumption that mean revolutionary stream surface (S1 surface) is cylinder, that is, inlet-exit axial velocity ratio is unity ( $AVR=1$ ). But in many actual conditions, the meridional streamlines are curved, the axial velocity ratio differs from unity ( $AVR \neq 1$ ) because of so many factors, such as stream surface inclination, growing boundary layers, radial pressure unbalance and so on. To employ the reliable experimental NACA cascade data and the conventional design procedure for  $AVR=1$  condition, it is necessary to transform the aerodynamic parameters under  $AVR \neq 1$  condition to those under  $AVR=1$  condition. Until now, though there are some local experimental statistical formulas evaluating the effect of AVR to the cascade performance [1] [2], but they can only be applied in some special conditions. Thus this paper tends to present a theoretical solution to the effect of the AVR on the cascade performance (flow angle, turning angle, equivalent diffusion ration, momentum thickness, total pressure defect coefficient) based on Schlichting theory. And through the comparison of the calculating flow angle data with the experimental ones, the accuracy of the derived singularity solution is also verified. With this method, a virtual-equivalent velocity diagram and NACA cascade data, an improved design procedure can be carried out. Its validity and reliability are also indicated by design examples which are have high performance.

## THE SINGULARITY SOLUTION TO THE EFFECT OF AVR ON THE CASCADE PERFORMANCE

On an averaged revolutionary stream surface (S1 surface), the relative movement equation satisfying stream function  $\psi$  can be given as follow:

$$\frac{\partial^2 \psi}{\partial m^2} + \frac{1}{r^2} \frac{\partial^2 \psi}{\partial \theta^2} + \left[ \frac{1}{r} \frac{\partial r}{\partial m} - \frac{1}{b\rho} \frac{\partial(b\rho)}{\partial m} \right] \frac{\partial \psi}{\partial m} - \frac{1}{b\rho} \frac{\partial(b\rho)}{r \partial \theta} = -2\omega b\rho \frac{\partial r}{\partial m} \quad (1)$$

According to Schlichting singularity theory [3], we transform the head induced by flow turning and centrifugal force with some distributed vortices and sources on the cascade row (Fig. 1), the intensity of the singularity series is given out by Glauert series:

$$r_b / w_{\infty x} = A_o \operatorname{ctg}(\theta / 2) + \sum_{j=2}^{n-1} B_j \sin(j\theta)$$

$$q_b / w_{\infty x} = B_o (\operatorname{ctg}(\theta / 2) - 2 \sin \theta) + \sum_{j=2}^n B_j \sin(j\theta) \quad (2)$$

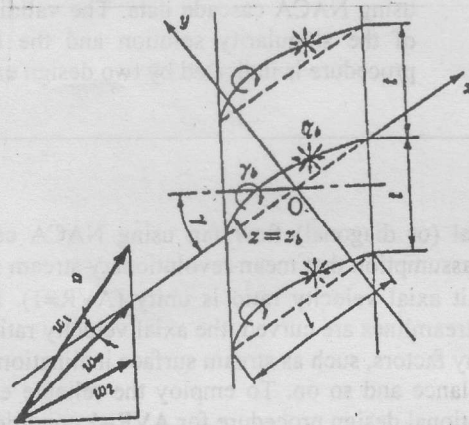


Figure 1: The distribution of singularity series.

The combination of the velocity field induced by the singularity series and the original velocity field should be meet the requirements of the local airfoil profile boundary. From this, the equations below hold for three points of a group in N groups of singularity:

$$\frac{A_o}{2} \left\{ -1 + w_{ryo}^* - \frac{dy_c}{dx} w_{rxo}^* \right\} + \sum_{j=1}^2 \left\{ \frac{A_j}{2} \left[ \cos(j\theta) + w_{ryj}^* - \frac{dy_c}{dx} w_{rxj}^* \right] \right\} + \frac{B_o}{2}$$

$$\left[ w_{qyo}^* - \frac{dy_c}{dx} (1 + 2 \cos \theta + w_{qxo}^*) \right] + \sum_{j=2}^3 \left\{ \frac{B_j}{2} \left[ w_{qyj}^* - \frac{dy_c}{dx} (-\cos(j\theta) + w_{qxj}^*) \right] \right\} \quad (3)$$

$$= -\xi / 2 \cos \theta / (1 + \operatorname{tg} \theta \operatorname{tg} \beta) (dy_c/dx + \operatorname{tg} \theta)$$

$$\frac{A_0}{2} \left\{ \frac{dy_d}{dx} w_{rxo}^* \right\} + \sum_{j=1}^2 \left\{ \frac{A_j}{2} \left[ \frac{dy_d}{dx} w_{rxj}^* \right] \right\} + \frac{B_0}{2} \left[ ctg\left(\frac{\theta}{2}\right) - 2 \sin \theta - \frac{dy_d}{dx} (-1 - 2 \cos \theta + w_{axo}^*) \right] + \sum_{j=2}^2 \left\{ \frac{B_j}{2} \left[ \sin(j\theta) - \frac{dy_d}{dx} (\cos(j\theta) + w_{axj}^*) \right] \right\} = -\frac{\xi}{2} \cos \theta / (1 + tg r tg \beta_x) \frac{dy_d}{dx} \tag{4}$$

Solve this 6N equations, get out the coefficient  $A_0, A_1$  of Glauert series, then the velocity circulation can be determined:

$$\Delta\Gamma / W_{\infty x} = \pi / 2 (A_0 + A_1 / 2) \tag{5}$$

By the virtual-equivalent velocity diagram (Fig. 2) [4], the flow angle and turning angle can be corrected, the equivalent diffusion ratio, momentum thickness, total pressure defect coefficient can be calculated also:

$$\begin{aligned} tg[\beta_1]_{corrected} &= (1 - \xi / 2) tg[\beta_1] + \Delta\Gamma / (2w_{\infty} t \cos \beta_{\infty}) \\ tg[\beta_2]_{corrected} &= (1 + \xi / 2) tg[\beta_2] - \Delta\Gamma / (2w_{\infty} t \cos \beta_{\infty}) \end{aligned} \tag{6}$$

$$D_{eq} = 1 / AVR \cos \beta_2 / \cos \beta_1 [1.12 + k_{\alpha} (\alpha A - \alpha^*)^{1.43} + 0.61 \cos \beta_2 / \sigma (tg \beta_1 - AVR tg \beta_2)] \tag{7}$$

$$\delta / L = \epsilon \{1 + K_A (AVR - 1)\} / (1 - K_s \text{Ln} D_{eq}) \tag{8}$$

$$\xi_p = 2(\delta/L) AVR \sigma / \cos \beta_2 \cos^2 \beta_1 / \cos^2 \beta_2 \tag{9}$$

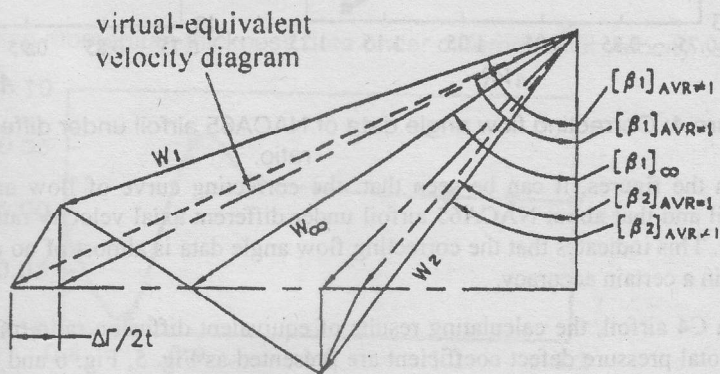


Figure 2: The virtual-equivalence velocity diagram.

## CALCULATIONG EXAMPLES

By the FORTRAN procedure programmed with the method above, a C4 airfoil and a NACA65 airfoil in case of  $\sigma = 1.0$ ,  $\beta_1 = 55^\circ$ ,  $\gamma = 45^\circ$  is calculated respectively, the results are showed as follow (Fig. 3, Fig. 4):

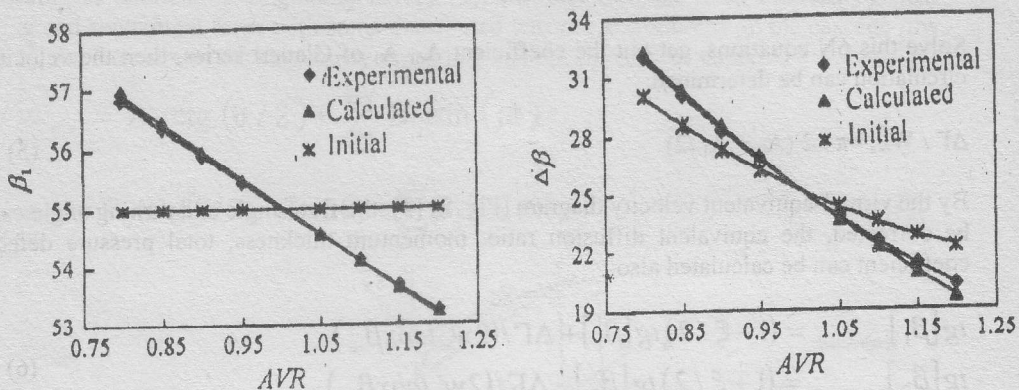


Figure 3: Correcting flow angle data of C4 airfoil under different axial velocity ratio.

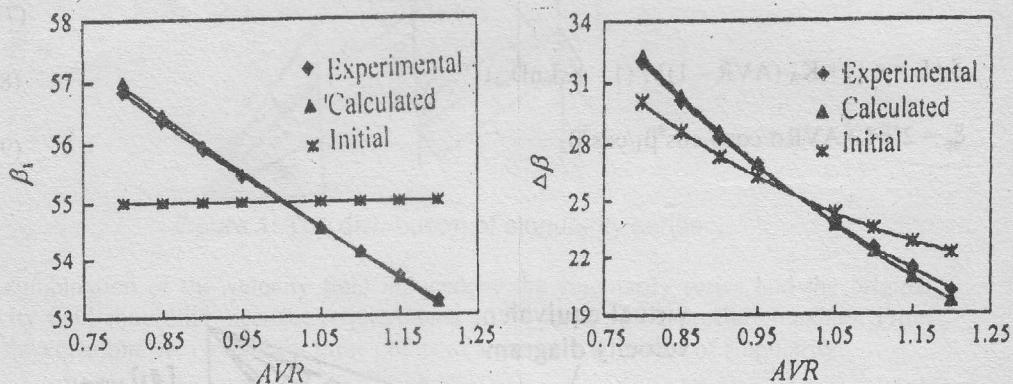


Figure 4: Correcting flow angle data of NACA65 airfoil under different axial velocity ratio.

From the figures, it can be seen that: the correcting curve of flow angle data about C4 airfoil and that about NACA65 airfoil under different axial velocity ratio are similar much more. This indicates that the correcting flow angle data is almost of no concern with airfoil type in a certain accuracy.

For a C4 airfoil, the calculating results of equivalent diffusion ratio, momentum thickness and total pressure defect coefficient are presented as Fig. 5, Fig. 6 and Fig. 7 respectively. According to the reference[5], the left part of  $Deq > 2.7$  in Fig. 5, the left part of  $AVR < 0.9$  in Fig. 6 and Fig. 7 are in range of stall. The decreasing abruptly and negative value of calculating data reveals the appearance of stall.

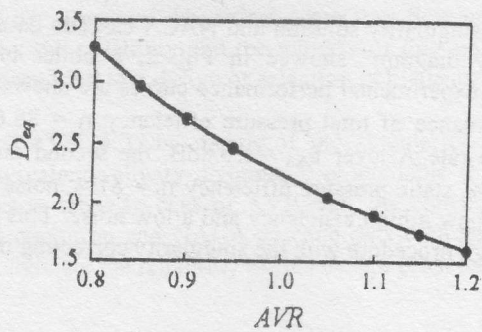


Figure 5: Correcting equivalent diffusion ratio data under different axial velocity ratio.

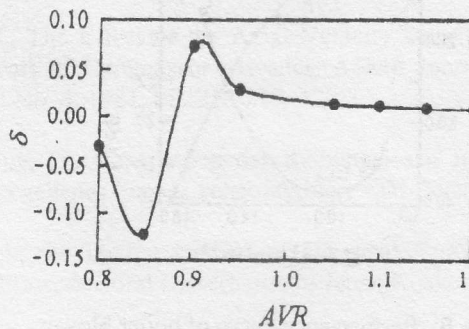


Figure 6: Correcting momentum thickness data under different axial velocity ratio.

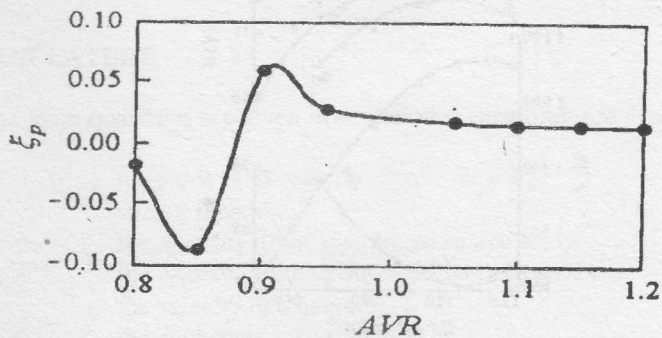


Figure 7: Correcting total pressure defect coefficient data under different axial velocity ratio.

## DESIGN EXAMPLES

Employing this theoretical singularity solution and NACA cascade data, together with the "virtual-equivalent velocity diagram" showed in Fig. 2, a boiler blower and a mine ventilator is designed. The experimental performance curves are showed in Fig. 8, Fig. 9. The first one has a performance of total pressure efficiency  $\eta = 88.6\%$ , static pressure efficiency  $\eta_t = 82\%$ , noise rate A lever  $L_{SA} = 16.8\text{dB}$ , the second one has that of total pressure efficiency  $\eta = 88\%$ , static pressure efficiency  $\eta_t = 81\%$ , noise rate A lever  $L_{SA} = 18.5\text{dB}$ . Both of the twos show a high efficiency and a low noise. This gives a good proof to the reliability of the design procedure with the singularity correcting method.

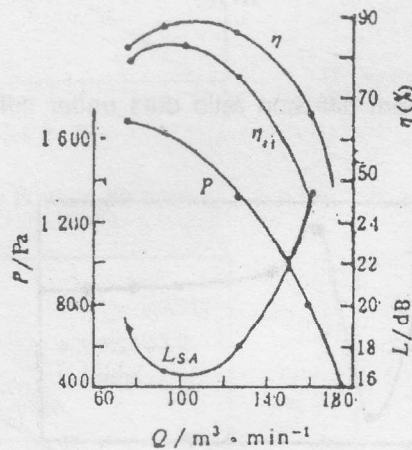


Figure 8: Performance curve of boiler blower.

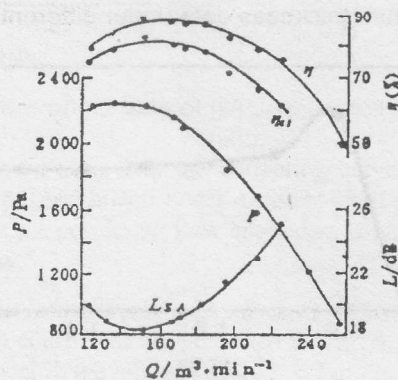


Figure 9: Performance curve of mine ventilator.

## CONCLUSION

- 1) The good agreement of theoretical correcting flow angle data with experimental ones shows the reliability and the validity of this singularity correcting solution, which is beneficial to a design or selection of blade airfoil.
- 2) In case of  $AVR \neq 1$ , by means of the singularity correcting solution and the virtual-equivalent velocity diagram, it is available to transform the aerodynamic parameters to those in case of  $AVR = 1$ , the conventional design system under  $AVR = 1$  condition and NACA cascade data then can be employed. The design examples indicate the reliability of this design procedure.

## REFERENCES

- [1] Yamaguchi., The Effect of Axial Velocity Ratio on the Deviation Angle of Blade Element in an cascade of Axial Velocity decreasing, Journal of Turbo-machine (Japanese) 1991, Vol. 19, No. 2, PP. 7-11.
- [2] Starke, J., The Effect of the Axial Velocity Density Ratio on the Aerodynamic Coefficients of Compressor cascades, ASME Journal of Engineering for Power Vol. 103, No. 4, 1981, PP. 210-219.
- [3] Schlichting, H., Berechnung der Reibungslosen Inkompressiblen Stromung fur ein, Vorgegebenes Ebenes Schaufelgitter, VDI-Forschungsheft, 447, 1955.
- [4] Wu Keqi., the Design method of Diagonal Fan and The Investigation of the Internal Flow, doctoral Dissertation of Japan Kushou University (Japanese), 1997.
- [5] Lieblein, S., Loss and Stall Analysis of Compressor Cascades, Trans. ASME ser. D. 81-3, 1959, P. 387.

## NOMENCLATURE

Only the main quantities are given here, the other quantities are explained in the reference [4].

AVR	:	inlet-exit axial velocity ratio, $= W_{z2}/W_{z1}$
$\psi$	:	stream function
$r_b$	:	the intensity of the distributed source series
$q_b$	:	the intensity of the distributed vortices series
$\Delta\Gamma$	:	the velocity circulation
$D_{eq}$	:	the equivalent diffusion ratio
$\delta$	:	the momentum thickness

$\xi_p$	:	the total pressure defect coefficient
$\sigma$	:	solidity, $L/t$
$\beta_1$	:	inlet flow angle
$\beta_2$	:	exit flow angle
$\gamma$	:	stagger angle
$\Delta\beta$	:	turning angle